Scanning Electrochemical Microscopy (SECM). Principles and Applications.

Fabian A. Rios

Department of Chemistry and Biochemistry, New Mexico State University, Las Cruces, New Mexico 88003

fabrios@nmsu.edu

RECEIVED DATE (to be automatically inserted after your manuscript is accepted if required according to the journal that you are submitting your paper to)

Principles, description and theory of operation modes and applications of Scanning Electrochemical Microscopy (SECM) are presented in this review. The main interest is to introduce the technique for the non-specialist and describe some of the fields were SECM has found widespread application since its invention in the late 80's.

1. Introduction

At the beginning of the 80's a new revolution began in microscopy [1], electromagnetic waves were no longer necessary to obtain images and now a probe was used to scan a surface an obtain a signal that could be translated into topographic information. The probe was commonly a tungsten or platinum-iridium wire that was chemically etched into a very fine tip. This idea gave born to the Scanning Tunneling Microscopy (STM), Atomic Force Microscopy (AFM) and some other similar techniques.

Almost at the same time, electrochemistry was also transformed by the apparition of ultramicroelectrodes (UME) [2, 7]. This new devices opened new possibilities in electrochemistry due to their unique properties associated with their small sizes. Not very long was necessary before somebody realized that UME's could serve as probes for a potential electrochemical microscope. Bard et

al, published their first paper describing some modes of the Scanning Electrochemical Microscopy (SECM) in 1989 and from that time on the development of this technique has been exponential [3].

SECM have found application in varied branches of electrochemistry such as electrocatalysis, mass transfer through interfaces, corrosion, bioelectrochemistry, etc. The main characteristics that have made it so useful are its high mass transfer coefficients, high spatial resolution, and precise theory that allow to extract accurately useful kinetic and mechanistic information [4, 5, 6].

The aim of this review is to present a concise description of SECM fundamentals. Basic instrumentation will be explore as well as the theory in the principal modes of operation of the microscope. Finally there will be a brief survey of the most relevant SECM applications.

2. Principles of SECM

2.1. Basic Instrumentation

Fig. 1 shows the block diagram of a common SECM set up. The main parts of the system are:

a) Electrochemical cell: three electrodes at least are needed for an SECM experiment, one reference, one counter and one working plus an optional electrode that correspond to the substrate. The first working electrode is an ultramicroelectrode (UME) which work as probe and will be described in a later section. The substrate electrode is optional since SECM it is not limited only to conductive samples.

The electrode system is controlled by a bypotentiostat which bias the potential of both working electrodes with respect to the reference. The main characteristic of this instrument must be its capacity to measure a broad range of currents and to have a high sensitivity since often the values of current trough the tip are of the order of nano and pico amps.

b) Positioner: it is a three-dimensional translational stage that allows to locate the tip with a high accuracy over the substrate. Modern equipments allow two kind of movements for tip using different

types of motors. Stepper motors for fast displacement and piezo controllers for high accuracy. The maximum resolution that can be obtained is of the order of 1.6 nm. For feedback mode of SECM only a postioner in the Z axis is necessary but for imaging an XYZ system must be assembled.

Due to the dimensions of the tip, vibration isolation is not a critical issue in SECM. Only for probes smaller than 10 μm it would be recommended to use air-tables, anti-acoustical boxes or some other mean of protection from external environmental noise that could excite some mechanical resonances [5].

c) Data acquisition and control system [5]: a significant amount of software is necessary to control the different features of an SECM experiment principally the recording of data and the positioning of the tip which must be done simultaneously. For the collection of current and voltage data from the electrochemical cell, especial routines must be implemented to maximize the signal-to-noise ration (SNR). The data system must be capable of recording very precise values in real time to allowed a good functioning of the tip positioning.

The control of the tip movement must be very precise too. This is particularly important when doing approach curves to avoid damaging of the probe. If the values of current are not send in real time to the control there is a high probability of breaking the UME.

For data analysis and display there are many commercial applications and normally programming is not necessary. Some of the basic routines needed to display images are tilt correction, least-square analysis, and interpolation.

d)Ultramicroelectrodes (UME): Since its apparition at the beggining of the 80's, the ultramicroelectrodes (UME's) created a whole revolution in electrochemistry [2]. These electrodes have the particular characteristic to have at least one dimension smaller than the diffusion layer generated during one experiment [4], such dimension must be < 25 μm.

Due to their particular small size the UME's present different advantages over regular size electrodes such as a fast steady state, low currents (which decrease the ohmic drop), high speed of response and

spatial resolution [8]. An stable steady state is especially useful in SECM since this allows to work without worries of transients which permit more accurate measurements and the acquisition of images.

Microelectrodes can have a number of different geometries, disk, hemispherical, cylindrical, microband, etc. However the most common type by far used in SECM is the disk UME. Disk UME's from 25 to 1 μm are routinely made from Pt, Au or Ag wire mainly. This wires are sealed in a glass capillary under vacuum and a connection is made with silver epoxy through a Cu wire. The disk is polished with sand paper first and finished with 1, 0.3 and 0.05 μm alumina. Specific instructions to make this electrodes can be found elsewhere [9]. Electrodes with much smaller dimensions have been made nonetheless, some of them with nanometer size down to 400 nm [10].

What makes a tip however it is the conical shape. The disk UME must be polished to decrease the area in the tip as much as possible. The relation between the radius of the electrode area and the total area is called RG. An UME with small RG can approach better and closer to the substrate increasing the quality of the measure current values. The conical tip has also become very popular since its mathematical modeling is more straightforward and most of the theory has been developed taking into account its geometry [5].

2.2. Modes of operation in SECM

The SECM setup allows different interactions between the tip and the substrate. Every one will present different analysis possibilities.

a)Feedback Mode: This mode is based on the measuring of the interaction of the tip when approaching a substrate. Figure 2 shows the possible interactions of the tip with the substrate.

There are basically three possibilities:

A. The tip is very far from the substrate: In this case the tip have a response of a normal UME because nothing is blocking the diffusion of R toward the surface. If the electrode is bias to a potential positive enough the oxidation of R takes place according to:

$$R \rightarrow O + ne^-$$

If the diffusional control is established the tip will reach the steady state. The value of the steady state current is given by [4]:

$$i_{ss} = 4nFDca$$

where n corresponds to the number of electrons transferred in the reaction, F is the Faraday constant, D is the diffusion coefficient of R, c is the concentration of the specie being reduced or oxidized at the substrate and a is the tip diameter.

B. Positive feedback: when the tip approaches a conductive substrate, depending of the potential at which this substrate is bias, there is the possibility to regenerate the species that are being oxidized on the tip. For example if the potential at the substrate is negative enough the following reaction will take place:

$$O + ne^- \rightarrow R$$

If this way the effective concentration of R in the gap between tip and substrate will increase and the current will reach a value larger than i_{ss} what is called the feedback. The closer the tip to the substrate, the better the feedback. Fig 3 (1) shows a typical positive feedback approach curve.

This type of curve can serve different purposes. First, it is an excellent way to determine if the setup is correctly configured. The values of current vs distance has been calculated using numerical simulations and approximated formulas proposed to adjust it with the experiment for different values of RG, which have been tabulated. The following is the resulting equation for RG=10 [11]:

$$I_T^C(L) = \frac{0.78377}{L} + 0.3315\exp\left(-\frac{1.0672}{L}\right) + 0.68$$

Where I_T is the ratio between the current of the tip and i_{ss} and L is the ratio between the distance from the substrate and the tip radius. Several other formulas can be found in the literature which try to be

more accurate or present a better description of the experiment [12] but for fast analysis formula 2 is useful enough.

Experimentally, the approach curve also serves to characterize the tip. Tip with different RG have different approach curves because once the glass sheath around the electrode becomes smaller the back diffusion of the electrochemical species increase its contribution to the measured current. In the same way, tips with different morphologies present characteristics profiles that can be used to estimate specific geometries [13].

Finally, the approach curve is the only method to place the tip at a known distance from the surface. This is especially useful when doing imaging and during generation-collection experiments.

C. No feedback mode: also called negative feedback. When the tip approaches an insulator substrate there is an effective blocking of the reduced species toward the tip causing a decrease in the i_{ss}. The type of curve obtained can be observed in figure 2 (2).

For this type of curve there is also numerical approximations being the most common [11]:

$$I_T^I(L)=\frac{١}{٠.٢٩٢}+\frac{1.5151}{L}+٠.٦٥٥٣\exp(-\frac{2.4035}{L})$$

Positive and negative feedback curves can be used for essentially the same purpose. However the negative feedback curve is more susceptible to the changes in tip geometry, especially in the value of RG. The following formula can be used to determine the influence of the RG.

$$I_T^{ins}(L)=\frac{1}{A+\frac{B}{L}+C\exp(\frac{D}{L})}+\frac{EL}{F+L}$$

Where the parameters A, B, C, D, E and F can be found elsewhere for different values of RG [13].

b) Collection modes

Both possibilities for this kind of operation are shown in figure 4. Only substrates that can generate an electrochemical specie can be used in this mode.

A. Tip generation substrate collection (TG/SC): for this case both currents, tip and substrate, are measured. The general idea is to position the tip to a certain distance from the substrate and observe the values of the current which will be affected by the feedback from the substrate and the diffusion from the gap between both electrodes. If the gap is small enough the collection efficiency must be almost one ($i_S/i_T > 0.99$). On the other hand if there are other reactions taking place this will affect the tip current and this variation will provide important kinetic information.

Fernandez et al. [14] introduced an interesting variation in the TG/SC mode when they used the tip in a galvanostatic mode (i.e. constant current). Situating the tip in a very close proximity to the substrate it was possible to measure the rate of reaction of species produces in the tip that do not generate a feedback, in their specific case oxygen in acid media. The main advantage of this approach was the stability on the generation of oxygen, since it is less affected by deactivation of the tip and an easier analysis of the data through the generation of simplified polarization curves.

B. Substrate generation tip collection: this technique was the precursor in the electrochemical microscopy field [15]. The tip was used to study the concentration profiles inside the diffusion layer which has a size of the order of microns. Short live species were detected in a much easier and accurate way than previous methods based on spectroscopic measurements close to the surface.

The tip in this mode of operation is used more as a sensor that disturb as little as possible the concentration profile, therefore the used of very small electrodes is very important and also a limiting factor.

c)Additional modes of operation [6, 19].

There are a number of additional operational modes in SECM, however they have found more limited application. For example, the ion-transfer feedback mode, described by Shao and Mirkin [16], utilizes a

micropipette electrode that induces ionic transport through and interface by depleting the concentration of in one of the two phases. Again, the high mass transfer coefficient of SECM and its spatial resolution plays a significant role in the measurement of rate constants as high as 1 cm/s.

The penetration mode is based on the study of electrochemical processes it the interior of very thin, non aqueous layers [17]. The SECM tip can reach this microenvironments and thanks to the capabilities of UME's to function in low conductive media, different redox reactions can be evaluated as if it were done in aqueous solutions.

Finally, the alternate current mode (ACSECM) uses impedance measurements to obtain local interfacial impedance properties with high lateral resolution [18]. This technique overcome the problems of "global" electrochemical impedance spectroscopy (EIS) which can only analyze large surface as an average while the most interesting processes in areas as corrosion and coating analysis, take place in discrete location like grain boundaries or microscopic defects.

3. Applications

3.1. Imaging [5]

Being the SECM a microscope the first use that must be mention is the acquisition of images. However in this field, SECM is a bit behind its cousins AFM, STM and other techniques that can provide much higher resolution. The resolution of an image in probe microscopy is largely determined by the size of the probe. Presently, the smaller tip that has been successfully fabricated border the range of hundreds of nanometers, giants compared with the atomic resolution of STM and AFM. An image of a Hep G2 cells while exporting Thiodine is shown in figure 5 as an example.

Imaging can be carried out in the different modes of SECM. The most simple approach is the imaging of nonconductive substrates. In this case the blockage of diffusion of the electrochemical specie in solution can be translated to topographic data when measuring the current of the tip.

SECM present an important advantage over its scanning probe counterpart and it is its capacity to differentiate substrates based on its reactivity. A technique called reaction rate-imaging, which is unique to SECM, is particularly useful in imaging the areas on a surface where reactions occur.

For example, positive feedback images has been used to identify zones of larger catalytic activity towards the hydrogen oxidation on highly oriented pyrolytic graphite (HOPG) that has been modified with Pt particles. It was possible to analyze different types of individual particles, at the same time, as a function of substrate potential [20].

The collection mode, as will be explained further on, has been especially useful in the collection of images of biological interest. For example, Scott et al, have been able to produce images of ionic transport through pores on mouse skin and determine that most of the movement of species takes place on pores associated with hair follicles [21]. Stomata in plant leaves have also been imaged through SECM. The upper surface of a *Ligustrum sinensis* leaf under illumination showed spots of higher oxygen concentration corresponding to indiviual stoma during respiration. With dark conditions the processes slow down to be recommenced upon illumination [22].

3.2. Electrocatalysis: SECM has proved to be useful in measuring of heterogeneous electron transfer. Its main advantage comes from the high mass transfer rates that can be obtained when the tip approaches the substrate as following equation states [5]:

$$m_o = 4D_o \frac{0.68 + \frac{0.78377}{L} + 0.3315\exp\left(-\frac{1.0672}{L}\right)}{\Pi a}$$

where m_o is the mass transfer coefficient. As can be seen, m_o depends on the distance from the substrate, the smaller the distance the higher the m_o. We can infer from here that the maximum kinetic reaction constant (k_o) that can be measure is of the order of D/d.

Kinetically controlled approach curves have also been mathematically adjusted, the same way than mass transfer controlled approach curves [23]. The formula is presented next:

$$I_T = I_S\left(1 - \frac{I_T^{ins}}{I_T^c}\right) + I_T^{ins}$$

$$I_s = \frac{0.78377}{L\left(1 + \frac{1}{\Lambda}\right)} + \frac{[0.68 + 0.3315\exp(-\frac{1.0672}{L})]}{[1 + F(L,\Lambda)]}$$

where I_s is the current of the substrate and Λ is the normalized kinetic constant. Adjusting the values corresponding to Λ one can obtain k_o for the electrochemical reaction.

To analyze the kinetics at the tip, this is held at a constant distance from the substrates and the potential scanned. The closer the distance the higher the mass transfer and the curves will proportionate information about the kinetics. The following aquation provides means to adjust the experimental data [24]:

$$I_T(E,L) = \frac{[٠.٦٨ + \frac{٠.٧٨٣٧٧}{L} + ٠.٣٣١٥\exp(-\frac{١.٠٦٧٢}{L})]}{(\Theta + \frac{١}{\kappa})}$$

$$\kappa = k^o \exp\frac{[-\alpha f(E - E^o)]}{m_o}$$

where E is the potential at the tip and α the transfer coefficient.

Application of this procedure has been very common. Zhou et al. [25] determined the kinetics of the proton reduction and hydrogen oxidation on platinum, a very fast reaction that have great importance in electrocatalysis. They found that the rate constants for these reactions were of the order of 0.37 cm/s. Using a similar procedure Liu et al. [26] measured the oxygen reduction in alkaline media using as complementary couple the hydroxide ion. The value obtained was 2 x10^{-3} cm s-1.

Recently Sun et al. [10], have shown the application of this technique for the measurement of very fast kinetics constants. Ru(hex) oxidation constant was measure obtainin around 17 cm/s with a 10nm nanoelectrode. The upper limit was set at 200 m/s.

One of the drawbacks of measuring kinetics with approach curves is that both, oxidized and reduced species, must form a couple that allows feedback. This is not the case when the hydrogen oxidation in basic media or the oxygen reduction in acid media are to be analyzed as is shown following:

$$H_2 + 2\mathrm{OH}^- \Leftrightarrow 2\mathrm{H}_2O + 2e^-$$

$$O_2 + 4\mathrm{H}^+ + 2e^- \Leftrightarrow 2\mathrm{H}_2O$$

as it is clear from the equation the specie at which H_2 is oxidized or O_2 is reduced is the solvent, H_2O. In this case, it is not possible to obtain feedback and other method must be found. Fernandez et al. [27] were able to use the TG-SC mode to generate maps of catalyst and determine their relative activity toward this kind of reactions. Figure 6 shows the method employed and a typical SECM image of an array of catalyst. Using this type of setup Fernandez et al. [28], were able to find a catalyst based on a combination of Pa-Co-Au which possesses equal or superior activity than Pt toward the hydrogen oxidation but is less costly.

3.3 Analysis of polymer thin films

SECM tip has been used to study some low density solid materials such as Nafion. Mirkin et al [17] were able to penetrate a very thin polymer film (aprox 200nm) using an extremely small, conically shaped Pt microelectrode tip (with a radius of 30 nanometers) . The experiment allowed to calculate the thickness of the film using an approach curve. Also the diffusion coefficient and the heterogeneous electron transfer for the reaction of $Os(bpy)_3^{2+}$ at the interior of the film were measured using the steady-state response at the UME.

Incorporation and release of ions from conducting polymer have been analyzed also. Yang et al. [29] were able to investigate the Electropolymerization, morphology characterization, and ion transport of poly(3,4-ethylenedioxythiophene) (PEDOT) films doped with different counterions (chloride, ferrocyanide (FCN), and poly(p-styrenesulfonate) (PSS-)) on a platinum electrode. They found that the incorporation and release of ionic species depends strongly of the applied potential to the polymer film.

3.4 Biological Applications [30, 31]

SECM has found a wide application on studies of model biological systems and cellular entities. Electron transfer measurements and transport of small molecules through interfaces are specially suitable for SECM due to its high spatial resolution and low disruption of the process that is analyzed.

3.4.1. Studies on cellular membranes analogous.

Physicochemical processes taking place at bilipid membranes are of paramount importance for the understanding of cellular functioning. Using monolayers (half of a bilayer) it has been possible to determine rates of electron transfer at the liquid-liquid interface and the air solid interface. Fig. 7 shows the possible processes that take place through a monolayer as can be sensed by a tip moving on top. Using this kind of setup Liu et al [32] was able to measure very fast heterogeneous (108 s^{-1}) and bimolecular (10^{11} mol^{-1} cm s^{-1}) electron transfer rate constants.

The uptake of molecules can be measured also as was shown by Baker et al [33]. In this application a submarine SECM tip was positioned below a monolayer at the air water interface as shown in figure 8. Maintaining the tip at a potential where the reduction of oxygen is under diffusion control, it was possible to evaluate the effects of the monolayer on the re-aireation rates, which is of significant importance in natural environments.

Studies of molecular transport and electron transfer have also been performed in bilayer lipid membranes (BLM) [34]. This type of membranes constitute the ultimate model for understanding the behavior of cellular membranes. Figure 9 shows the schematic apparatus used to measure ionic and and redox currents. The permeation of $Ru(NH3)_6^{3+}$, $Fe(CN)_6^{3-}$ and I^- through the ion channels in the

BLM was investigated and reported. Using a four-electrode system, potentials were applied across the membrane, to facilitate opening of the channels which occurred at a membrane potential of 50 mV. The number of alamethicin molecules forming an average channel was determined by monitoring the dependence of the total ionic current on alamethicin concentration.

3.4.2. Experiments with living cells.

SECM has been used to monitor the generation and consumption of chemical species from a living cell. Oxygen is perhaps the most used specie because its concentration around a group of cells it is a clear indication of their health and a proof of the well functioning of their metabolism. Different experiments has been carried out monitoring oxygen concentration around a cell after exposure to chemical agents or drugs. For example, Torisawa et al. [35] evaluated the effect of an anticancer drug in different kinds of cells. Using the imaging capabilities of SECM they were able to measure continuously the invivo-like condition of the cells after exposure to 1 μM of ADM.

Holt et al also [36] followed the cell metabolism after exposing E. Coli bacterias to minute amounts of $AgNO_3$. They found that the addition of concentrations of Ag^+ smaller than 10 μM are able to disrupt cell respiration causing an increase before death. This study permitted to evaluate then the antibacterial activity of Ag.

Other type of experiments with in vivo cells have to deal with the analysis of redox reactions inside the cytoplasm. Liu et al. [38] probe the redox activity of individual mammalian cells using a redox mediator capable of crossing the cell membrane. The processes could be represented as follows:

$$O + ne^- \rightarrow R \quad (at\ the\ tip)$$
$$R + O_{cell} \rightarrow R_{cell} + O \quad (inside\ the\ cell)$$

The tip was positively bias and moved toward the cell. The feedback curves were adjusted to the theory and the rate constant extracted. Using this procedure was possible to identify significantly differences in the activities of cells which differ in their metastatic state.

Finally, it will be important to mention the measurement of transport of species through the cellular membrane. Using SECM, Mauzeroll et al [38] were able to measure the uptake of menadione by yeast cells. Thiodine, the product of this reaction, was detected at the tip. A flux of around 30000 molecules

s^{-1} was measured using a 1 μm tip. In this experiments, the results was averaged over a large number of yeast cells since the size of them is much smaller than the size of the probe.

4. Conclusions

SECM is an electroanalytical technique that has developed exponentially during the last years. In this review some but not all of the most interesting applications has been described. There is still a wide range of problems where SECM has shown its applicability and this trend will continue in the years to come. Thanks to the advances in electronic and miniaturization the scope of the analysis that can be done will spread still more, especially in the field of bioelectrochemistry where SECM is a useful tool to explore cell metabolism.

5. Bibliography

[1] Binning, G.; Rohrer, H.; Gerber, C.; Weibel, E.; Phys. Rev. Lett., **1982,** 49, 57-61.

[2] Wightman, R. M. ; Anal. Chem., **1981,** 53, 1125A.

[3] Bard, A. J.; Fan, F. F.; Kwak, J.; Lev, O.; Anal. Chem., **1989**, 61, 132.

[4] Electrochemical Methods, Fundamentals and Applications. Bard, A. J.; Faulkner, L. R.; Marcel Dekker, New York, 2001.

[5] Scanning Electrochemical Microscopy. ed. A. J. Bard and M. V. Mirkin, Marcel Dekker, New York, 2001.

[6] Sun, P.; Laforge, F.; Mirking, M. V.; Phys. Chem. Chem. Phys., **2007,** 9, 802-823.

[7] Dayton, M. A.; Brown, J. C.; Stutts, K. J.; Wightman, R. M.; Anal. Chem. **1980,** 52, 946-950.

[8] Aoki, K.; Electroanalysis, **1993**, 5, 627-639.

[9] Zoski, C.; Electrocatalysis, **2002,** 14, 1041-1051.

[10] Sun, P.; Mirkin, M.; Anal. Chem. **2006,** 78, 6526-6534.

[11] Amphlett, J.; Denuault, G.; J. Phys. Chem. B, **1998**, 102, 9946-9951.

[12] Lefrou, C.; J. Electroanal. Chem., **2006**, 592, 103-112.

[13] Zoski, C.; Liu, B.; Bard, A.; Anal. Chem., **2004**, 76, 3646-3654.

[14] Fernandez, J.; Bard, A.; Anal. Chem. **2004**, 76, 2281-2289.

[15] Engstrom, R. C.; Weber, M.; Wunder, D.; Burgess, R.; Winquist, S.; Anal. Chem. **1986**, 58, 844-848.

[16] Shao, Y. ; Mirkin, J.; Phys. Chem. B, **1998**, 102, 9915.

[17] Mirkin, M.; Fan, F.; Bard, A. J.; Science, **1992,** 257, 354.

[18] Ballesteros, B.; Schulte, A.; Calvo, E. J.; Koudelka-Hep, M.; Schuhmann, W.; Electrochem. Comm., **2002**, 4, 134–138.

[19] Lu, X.; Wang, Q.; Liu, X.; Anal. Chim. Acta., **2007**, 601, 10–25.

[20] Kucernak, A. R.; Chowdhury, C. P.; Wilde, C. P.; Kelsall, G. H.; Zhu, Y. Y.; Williams, D. E.; Electrochim. Acta., **2000**, 45, 4483.

[21] Scott, E. R.; White, H. S.; Phipps, J. B.; Anal. Chem. **1993**, 65, 1537-1545.

[22] Tsionsky, M.; Cardon, Z.; Bard, Allen J.; Jackson, R. B., Plant Physiol., **1997**, 113, 895-901.

[23] Mirkin, M. V.; Fan, F.-R. F.; Bard, A. J.; J. Electroanal. Chem., **1992**, 328, 47.

[24] Bard, A. J.; Fan, F.; Mirkin, M.; Electroanal. Chem., **1994,** 18, 243.

[25] Zhou, J.; Zu, Y.; Bard, A. J.; J. Electroanal. Chem., **2000,** 491, 22–29.

[26] Liu, B.; Bard, A. J.; J. Phys. Chem. B., **2002**, 106, 12801-12806.

[27] Fernandez, J.; Bard, A. J.; Anal. Chem., **2003**, 75, 2967-2974.

[28] Fernandez, J.; Walsh, D. A.; Bard, A. J.; J. Am. Chem. Soc., **2005**, 127, 357-365.

[29] Yang, N.; Zoski, C.; Langmuir; **2006**, 22, 10338-10347.

[30] Roberts, William S.; Lonsdale, Daniel J; Griffiths, John; Higson, Seamus P.J.; Biosens. Bioelectron., **2007**, 23, 301–318.

[31] Edwards, Martin A.; Martin, Sophie; Whitworth, Anna L.; Macpherson, Julie V.; Unwin, Patrick R.; Physiol. Meas., 2006, 27, R63–R108.

[32] Liu, B.; Bard, Allen J.; Mirkin, Michael V.; Creager, Stephen E.; J. Am. Chem. Soc., **2004**, 126, 1485-1492.

[33] Barker, Anna L.; Gonsalves, Marylou; Macpherson, Julie V.; Slevin, Christopher J.; Unwin, Patrick R.; Anal. Chim. Acta., 1999, 385, 223-240.

[34] Matsue, T.; Shiku, H.; Yamada, H.; Uchida, I.; J. Phys. Chem., **2004**, 98, 11001–11003.

[35] Torisawa, Yu-suke; Kaya, Takatoshi; Takii, Yuki; Oyamatsu, Daisuke; Nishizawa, Matsuhiko; Matsue, Tomokazu; Anal. Chem., **2003**, 75, 2154-2158.

[36] Holt, Katherine B.; Bard, Allen J.; Biochemistry, **2005**, 44, 13214-13223.

[37] Liu, B.; Rotenberg, A. A.; Mirkin, M. V.; Anal. Chem., **2002**, 74, 6340.

[38] Mauzeroll, J.; Bard, A. J.; Proc. Natl. Acad. Sci. U.S.A., **2004**, 101, 7862.

[39] Amemiya, Shigeru; Guo, Jidong; Xiong, Hui; Gross, Darrick A.; Anal. Bioanal. Chem., 2006, 386, 458–471.

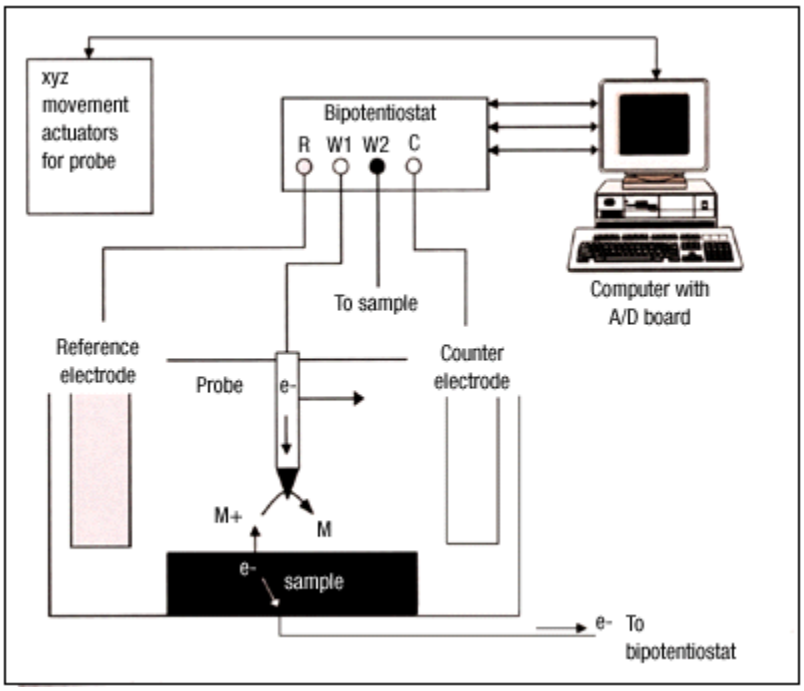

Figure 1. Schematics of SECM setup.

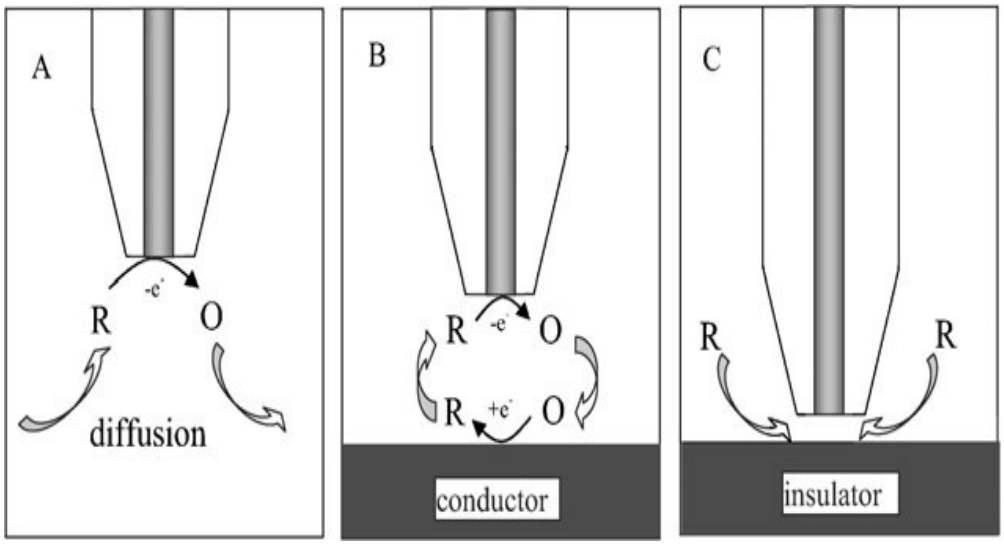

Figure 2. Possible tip interaction with substrate in feedback mode of SECM. A. Far from the substrate. B. Positive feedback. C. No Feedback.

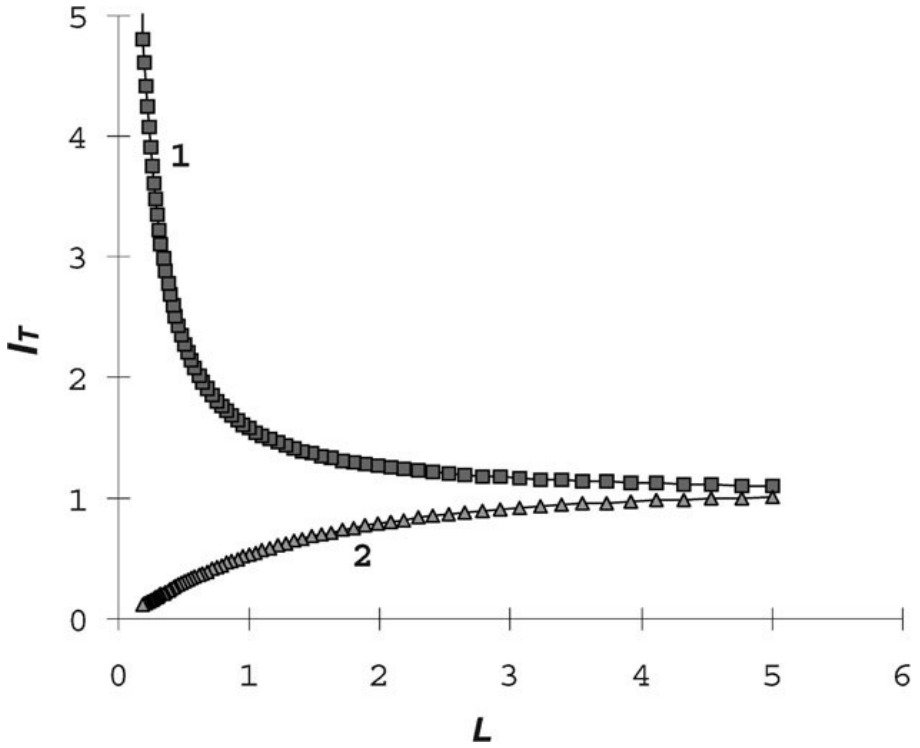

Figure 3. Approach curves to a substrate in SECM. Curve 1. Positive feedback approach curve – mass transfer control. Curve 2. Negative feedback approach curve.

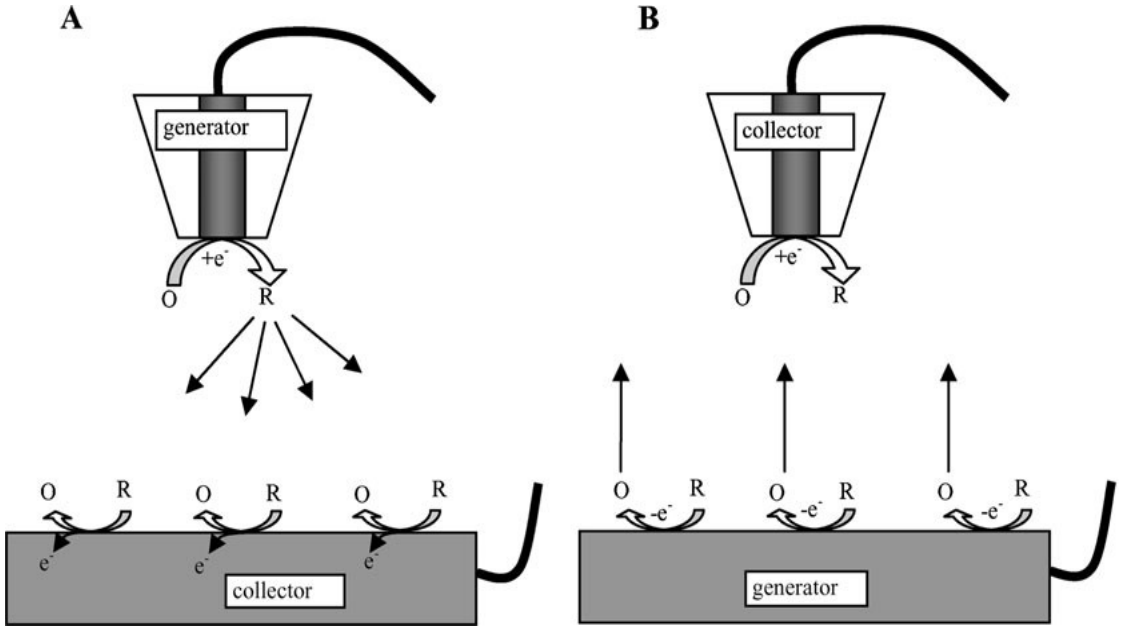

Figure 4. Collection modes of SECM. A. Tip Generation – Substrate Collection (TG-SC). B. Substrate Generation – Tip Collection (SG-TC).

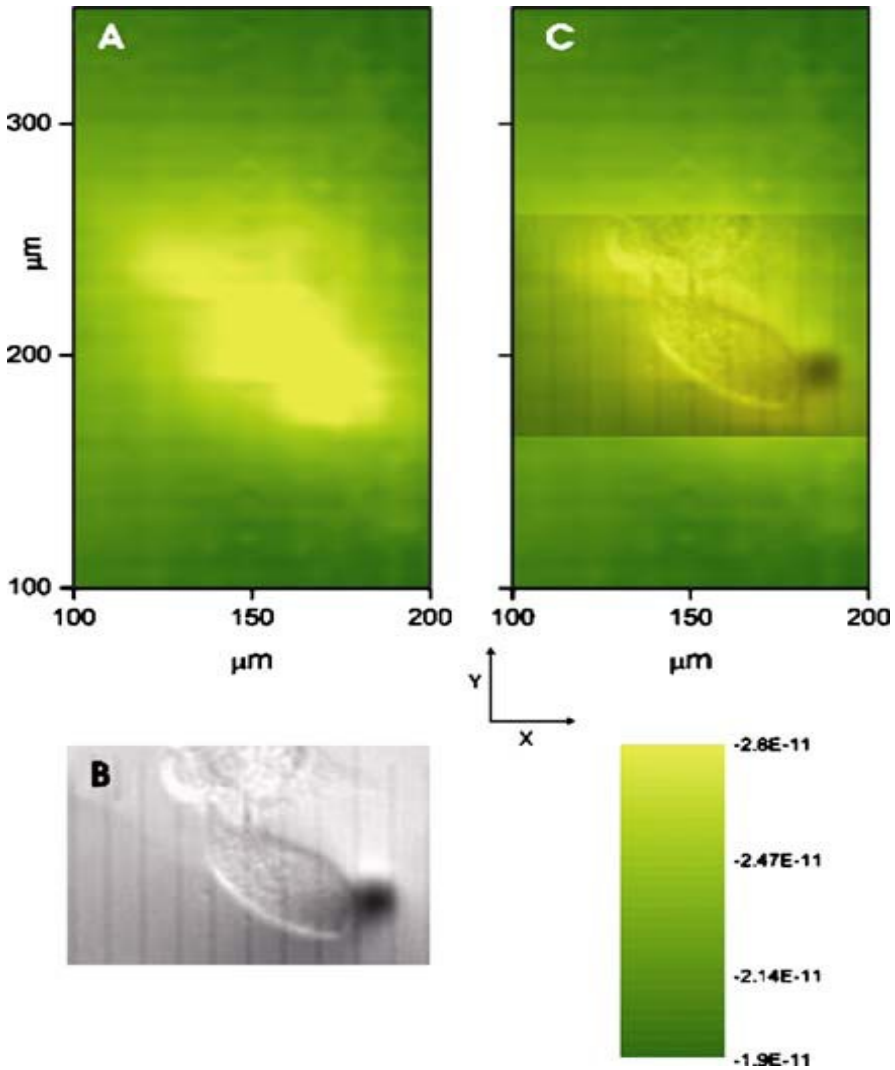

Figure 5. A SECM image of the export of thiodione from two neighboring Hep G2 cells, as detected using a 10-µm Pt UME. B Simultaneous optical micrograph of the Hep G2 cells being imaged. c Superimposed transparent optical micrograph on the SECM image from Ref 39.

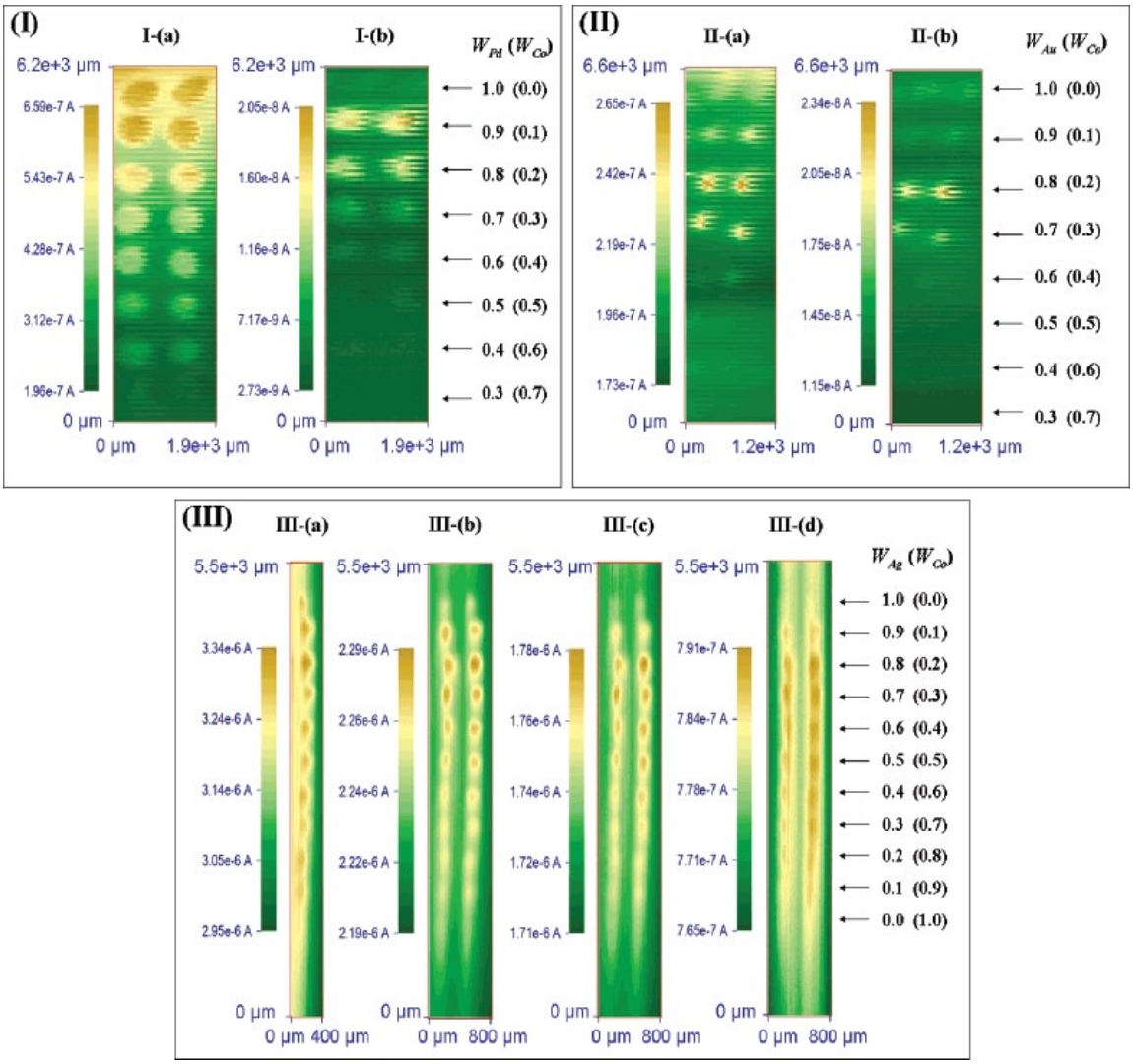

Figure 6. SECM TG-SC images of oxygen reduction activity measured on binary arrays in 0.5 M H2SO4. Tip-substrate distance) 30 ím, tip current) -160 nA. (I) Pd-Co, scan rate) 50 ím each 0.2 s, ES) 0.4 (I-a), 0.7 (I-b) V vs HRE; (II) Au-Co, scan rate) 50 ím each 0.2 s, ES) 0.2 (II-a), 0.4 (II-b) V vs HRE; (III) Ag-Co, scan rate) 20 ím each 0.017 s, ES) -0.05 (III-a), 0.05 (III-b), 0.15 (III-c), 0.2 (III-d) V vs HRE. WM is the atomic ratio of metal M in the spot. From Ref 28.

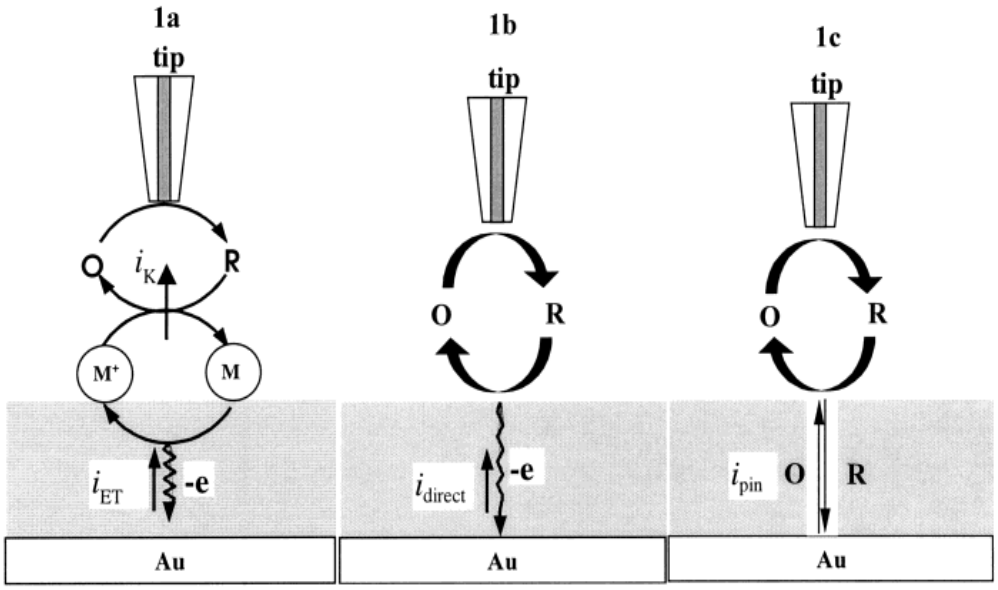

Fig 7. Schematic view of the processes involved in the SECM measurements of ET across an electroactive SAM: (a) mediated ET; (b) direct electron tunneling through monolayer; (c) ET through pinholes. From Ref 32.

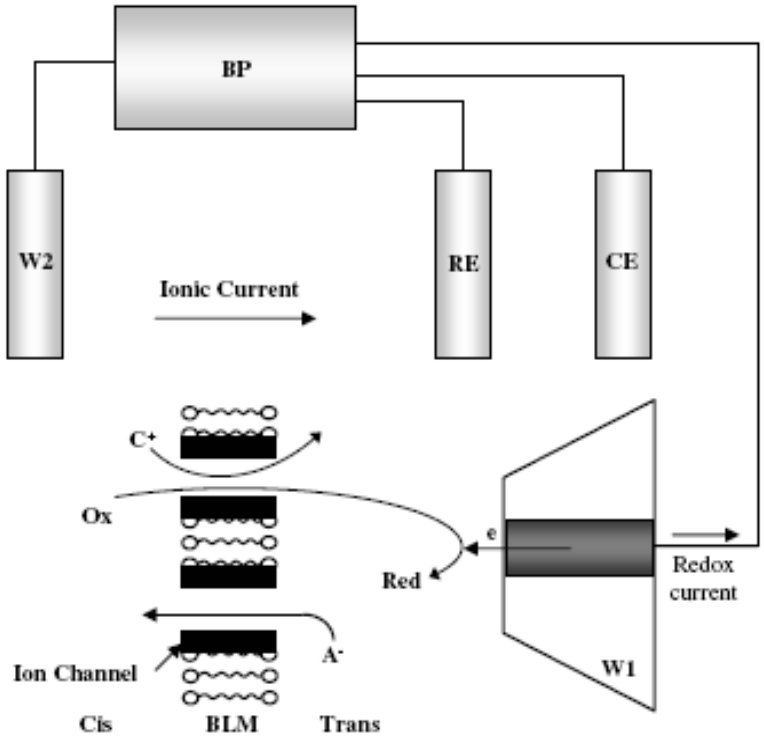

Figure 9. Schematic of the apparatus used to make simultaneous ionic and redox current measurements of transport across a BLM. BP = bipotentiostat; W1 = Pt microdisc electrode; W2 = Ag/AgCl electrode; RE = Ag/AgCl connected to virtual ground; CE = Pt wire. From Ref 31.